Tutor/s

Dr. Jordi Ignés- Mullol
Departament de Ciència de Materials i Química Física

Dr. Carlos Rodríguez-Abreu
Dr. Santiago Grijalvo
IQAC-CSIC
CIBER BBN

Grau de Química

Treball Final de Grau

Preparation of Antioxidant-Loaded Polymeric Nanoparticles towards a novel Therapeutic Strategy for Alzheimer's Disease.

Preparació de Nanopartícules Polimèriques Carregades amb Antioxidants com a nova Estratègia Terapèutica pel Tractament de l'Alzheimer.

Luna García Muñoz

June 2021

UNIVERSITAT DE BARCELONA

B:KC Barcelona Knowledge Campus
Campus d'Excel·lència Internacional

Los García Muñoz siempre llegan.

Mama

Donar les gràcies al Dr.Santiago Grijalvo per tota l'ajuda brindada durant la realització d'aquets treball i per la seva gran vocació i immillorable tasca com a tutor. Molt agraïda també a tot el grup de Química Col·loidal i Interfacial de l'IQAC per la seva gran acollida, en especial als meus companys de laboratori Joan, Marc, Riccardo, Luca, Laura i Lou-Anne per treure'm sempre un somriure.

Per últim agrair a la família i amics per haver estat al meu costat durant aquets quatre anys. Amanda, Maria i Júlia no ho hauria aconseguit sense vosaltres.

REPORT

CONTENTS

1. SUMMARY

Nanotechnology is nowadays an encouraging technology for novel therapies on non-communicable diseases (NCDs) such as cancer or Alzheimer (AD).

Current treatments for these diseases lack efficiency, mostly due to sluggish passage of the drugs through the blood-brain barrier (BBB). Development of biocompatible nanoparticles has allowed improved drug delivery systems with very low toxicities, great BBB permeabilities and enhanced delivery of poorly water-soluble drugs.

Although AD pathological pathways are still not fully comprehended, it has been noted that molecules that account for high antioxidant and anti-inflammatory activities reduce AD's progress. Among these substances we can find ferulic acid (FA), an abundant hydroxycinnamic acid present in cell wall complexes of plants that has been proven to hold neuroprotective capacities that alter amyloid-β (Aβ) fibril formation and protect the brain from Aβ neurotoxicity.

Aβ fibril accumulation and Aβ plaque formation are thought to be one of the major causes of AD, thus strategies targeting its disaggregation are crucial in the development of the latest treatments.

During this work carried out at the IQAC Colloidal and Interfacial Chemistry group led by Dr.Carlos Rodríguez, poly(lactic-*co*-glycolic acid) (PLGA) FA-loaded NPs were prepared and optimised by nano-emulsion templating to evaluate the NPs capacities for AD therapies.

A variety of techniques were used to assess nanoparticle's properties, including hydrodynamic diameter, surface charge, FA's release, cytotoxicity, antioxidant effects and interactions with Aβ peptide.

Key words: Aβ protein, Alzheimer disease, Drug delivery Systems, Ferulic acid, Nanocarriers, Nanoparticles, PLGA.

2. RESUM

La nanotecnologia suposa avui dia una eina molt prometedora pel desenvolupament de noves teràpies pel tractament de malalties no transmissibles (ENT) com ara el càncer o l'Alzheimer (AD).

Les teràpies actuals però, no són prou eficaces, principalment degut al pas limitat dels fàrmacs a través de la barrera hematoencefàlica (BHE). El desenvolupament de nanopartícules biocompatibles ha permès millorar els sistemes de distribució dels fàrmacs, augmentant així la permeabilitat de les drogues a la BHE i mantenint uns nivells de toxicitat molt baixos. També han suposat una gran millora en la distribució de fàrmacs poc solubles en aigua.

Tot i que les vies patològiques de l'AD encara no es comprenen del tot, s'ha observat que les molècules que presenten activitats antioxidants i antiinflamatòries elevades redueixen el progrés de la malaltia. Entre aquestes substàncies podem trobar l'àcid ferúlic (FA), un àcid hidroxicinàmic molt abundant present en els complexos de la paret cel·lular de les plantes que s'ha demostrat que presenta capacitats neuroprotectores que alteren la formació de fibril·les β-amiloides (Aβ) i protegeixen el cervell de la neurotoxicitat Aβ.

Es creu que l'acumulació de fibril·la Aβ i la formació de plaques Aβ són una de les principals causes de de l'AD, per això les estratègies dirigides a la seva desagregació són crucials per al desenvolupament dels darrers tractaments.

Durant aquest treball realitzat al grup IQAC de Química Col·loidal i Interfacial dirigit pel Dr. Carlos Rodríguez, es va preparar i optimitzar la formulació de NPs de poly(lactic-*co*-glycolic acid) (PLGA) carregades amb FA mitjançat templating de nano emulsions per avaluar les capacitats d'aquestes per a teràpies contra l'AD.

Es van utilitzar diverses tècniques per avaluar les propietats de les nanopartícules, entre les quals el diàmetre hidrodinàmic, la càrrega superficial, l'alliberament de FA, la citotoxicitat, els efectes antioxidants i les interaccions amb el pèptid Aβ.

Paraules clau: Proteïna Aβ, Alzheimer, Àcid ferúlic, nanotransportadors, nanopartícules, PLGA.

3. INTRODUCTION

Nanotechnology applications are countless and very promising. This multidisciplinary field incorporates science, technology of materials and engineering on a nanometric scale and allows new approaches to modern medicine challenges on non-communicable diseases (NCDs) such as cancer or Alzheimer (AD).

Current treatments for these diseases lack efficiency, mostly due to difficulties faced by the drugs in crossing the brain-blood barrier (BBB) and penetrating the central nervous system (CNS). Development of nanotechnology has achieved improved drug delivery systems consisting in biocompatible nanoparticles which display very low toxicities, great BBB permeabilities and improved delivery of poorly water-soluble drugs.

Nanoparticles (NPs) are small colloidal non thermodynamically stable systems with unique physical and chemical properties and large area to volume ratios. Their reactivity and properties are dependent on size, shape and structure and they can be prepared from a wide range of materials such as polymers, carbon, or lipids.

Amongst nanometric carriers, polymeric NPs made up of biodegradable polymers have received great interest on account of their high loading capacities, long circulation half-life and possibility of surface functionalization. The most widely used biocompatible polymers are polylactic acid (PLA) and poly(lactide-*co*-gycolide)(PLGA)(Figure 1).

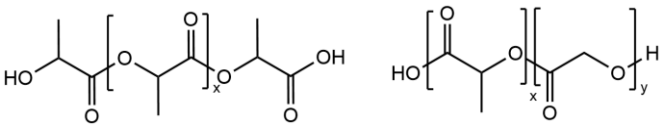

Figure 1. Polylactic acid polymer (PLA, left) and poly(lactide-*co*-gycolide) (PLGA, right).

Polymeric nanoparticles can be prepared by nano-emulsion templating. High energy methods have commonly been used for nano-emulsion preparations, however high energy requirements

for nanometric droplet formation are very cost-inefficient. Low energy emulsification methods on the other hand, make use of the internal chemical and surface energy of the system for the preparation of nanoparticles and enable formation of smaller droplet sizes.

Among low-energy emulsifying methods, the phase inversion composition method (PIC) relies on the phase transitions during emulsification process at constant temperature (Figure 2). Steady addition of the water phase (W) onto the oil phase (O) at constant temperature induces spontaneous change in the surfactant's curvature (W/O to O/W emulsion) enabling formation of nano-emulsions with low polydispersity and small droplets size[1]. If the polymer can be dissolved in a volatile oil phase, i.e. a hydrophobic solvent dispersed as droplets in the nano-emulsions, evaporation of this solvent will result in the formation of polymeric nanoparticles through a templating mechanism. This method was chosen for NPs preparation as will be shown later in this work.

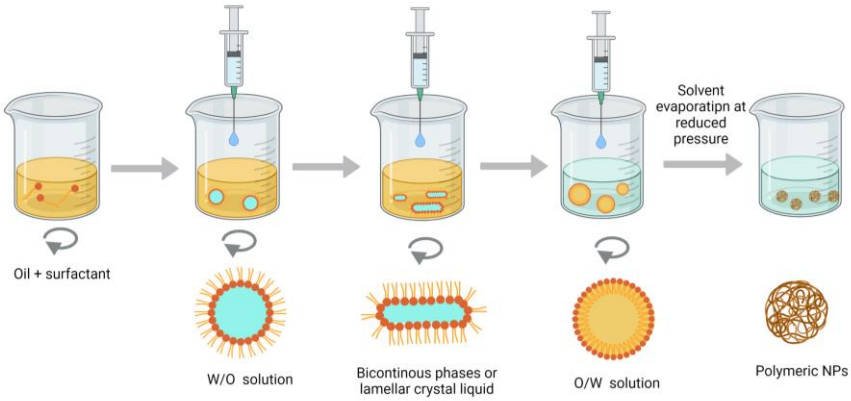

Figure 2. NPs formation by the phase inversion composition method (PIC).

3.1. ALZHEIMER DISEASE

Nanometric carriers are an encouraging technology for novel therapies against neurodegenerative diseases such as AD. This condition is an age-related neurodegenerative disorder that affects a worldwide population of over 37 million people[2]. Patients suffering from this affection experience gradual memory loss, confusion, apraxia, and general decline in cognitive function.

Because of its vast presence in nowadays fast-aging society, strategies for AD therapy are being actively researched. Several factors such as oxidative stress, deposition of amyloid-β (Aβ), Aβ plaque formation in the brain, intraneuronal accumulation of hyperphosphorylated tau protein, and low levels of acetylcholine are thought to play a major role in AD although pathological pathways of the disease are still not fully comprehended[3].

Two major hypotheses on the molecular mechanisms of AD have been suggested: (i) amyloid cascade hypothesis and (ii)Tau hypothesis, among others. In recent years, there is mounting evidence that these markers may appear many years before the onset of cognitive symptoms of the disease hence they constitute an interesting tool for diagnosis, control, and treatment of AD.

3.1.1. Amyloid cascade hypothesis

The amyloid cascade hypothesis suggests that the neurodegenerative process in AD is caused by a series of events triggered by the abnormal behaviour of the amyloid precursor protein (APP) which induces the production, aggregation, and deposition of toxic amyloid-beta (Aβ) in the extracellular matrix of neuronal cells[4].

Amyloid-beta protein is a cleavage product of the amyloid precursor protein, a transmembrane protein mainly present in neuronal and glial cells of the brain. APP is sequentially cleaved by two membrane-bound endoproteases, β- and γ-secretase (Figure 3). Cleavage by γ-secretase is imprecise and results in generation of Aβ protein.

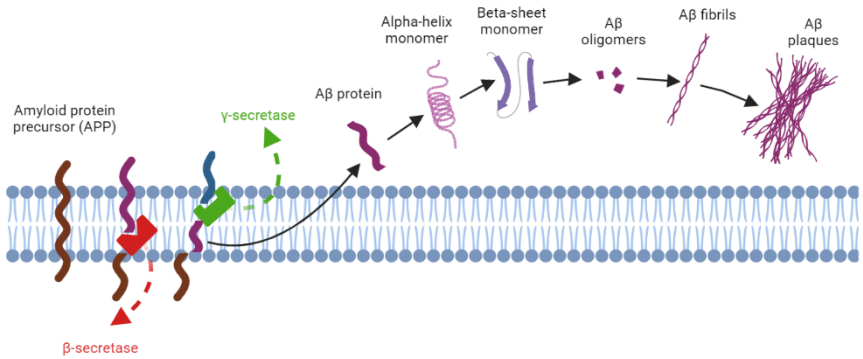

Figure 3. Cleavage of precursor protein (APP) followed by formation and plaque aggregation of Aβ fibrils.

Numerous different Aβ species exist, being $A\beta_{1-42}$ the longest, most hydrophobic and fibrillogenic thus the most fatal due to its great aggregation capacity and extreme neurotoxicity.

3.1.2. Tau hypothesis

Tau hypothesis states that tau tangle pathology is the main cause of AD. Tau is a cytoskeletal microtubule-associated protein present in the neurons and central nervous system. Phosphorylation of this protein reduces microtubule assembly and in hyperphosphorylation conditions tau protein self-assemblies into helical straight filaments. Oligomerization of these structures induces sedimentation of insoluble cluster structures known as NFT. Insoluble NFT hinders nervous signal transmission between neurons resulting in cell apoptosis (Figure 4).

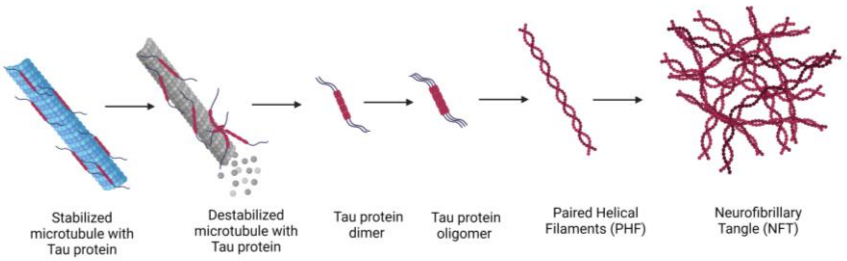

Figure 4. Phosphorylated tau protein destabilizes and aggregates into helical filament (PHF), eventually forming neurofibrillary tangles (NFT).

Drugs belonging to the family of acetylcholinesterase inhibitors (donepezil, rivastigmine), glutamate receptor antagonists (galantamine and memantine) and N-methyl-D-aspartate (NMDA) receptor have been administered to attenuate AD's symptoms and have shown positive effects against the disease[5]. Nonetheless, current available therapies for AD only reduce the severity of symptoms but are unable to cure the disease.

3.2. FERULIC ACID POTENTIAL AS A THERAPEUTIC AGENT FOR AD

Aβ plaque formation in specific regions of the brain induces neuroinflammation and free radical production as well as increased levels of oxidative markers. Free radicals like reactive

oxygen species (ROS) are prone to interact and cause damage to all types of lipids, especially in the brain[6], so antioxidant substances reducing oxidative stress play an important role in AD's progression.

Polyphenols are one of the most important groups of natural metabolites of plants and possess antioxidant and anti-inflammatory properties long time acknowledged by the scientific community. Substances such as curcumin, caffeic acid, rosmarinic acid (RA) or ferulic acid (FA) have shown to hold neuroprotective capacities that alter Aβ fibril formation and protect the brain from Aβ neurotoxicity[3,6].

FA is the most abundant hydroxycinnamic acid in the plant world (Figure 5). It is found in most higher plants as one of the key components in the cell wall complex[7] and accounts for high antioxidant and anti-inflammatory activities[8]. Its capacity for free radical scavenging resides in its chemical structure; FA phenolic ring and conjugated side chains enable the formation of resonance stabilized phenoxy radicals.

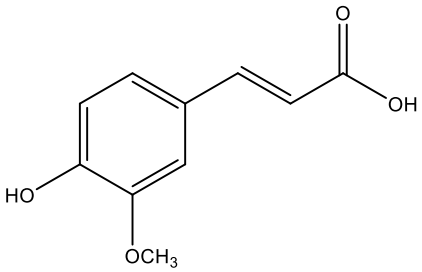

Figure 5. FA structure.

The presence of a carboxylic acid and phenolic functional groups in FA also provides chemical space for multiple structural modifications. In fact, several FA-based hybrids are under investigation as multi-target directed ligands (MTDLs) to develop new compounds for the treatment of AD[2].

Given its vast potential, FA is widely used in food, cosmetics, and pharmaceutical industries, however its applicability as a drug is constrained due to its low water solubility and sluggish entry into the brain through the BBB. Encapsulation of FA in nanometric carriers ought to be a promising strategy to overcome aforesaid limitations and improve current AD therapies while preventing FA's degradation in the blood stream.

4. OBJECTIVES

This undergraduate thesis has been carried out in the IQAC Colloidal and Interfacial Chemistry group led by Dr.Carlos Rodríguez. The main purpose of this work has been to study potential applications of FA-loaded NPs as therapeutic systems for AD treatment. The specific objectives have been:

1) Nano-emulsion templating and synthesis of FA-loaded PLGA NPs following a previously optimised PIC method[9].
2) Optimisation of NPs formulation (hydrodynamic diameter, surface charge and encapsulation efficiency).
3) Drug release studies to assess FA's liberation rate when encapsulated in PLGA NPs.
4) *In vitro* studies: Evaluation of cytotoxicity, antioxidant effects and interactions with amyloid peptide of the FA-loaded NPs.

5. EXPERIMENTAL SECTION

5.1. MATERIALS AND METHODS

Poly(lactic-*co*-glycolic acid; PLGA) with an average molecular weight of 10000 $g \cdot mol^{-1}$ was purchased from Boehringer Ingelheim (Ingelheim am Rhein, Germany). Polysorbate 80 (Tween 80), a derivate from polyethoxylated sorbitan and oleic acid, as well as FA and $A\beta_{1-42}$ peptide were purchased from Merck Sigma-Aldrich (Saint Louis, MO, USA). Ethanol and ethyl acetate were purchased from Panreac (Darmstadt, Germany) and were used as received. Water was MiliQ filtered (Millipore) (Massachusetts, MA, USA). A phosphate-buffered saline (PBS 1X) solution was obtained from sodium chloride (NaCl), potassium chloride (KCl), disodium monohydrogenphosphate dihydrate ($Na_2HPO_4 \cdot 2H_2O$) and potassium dihydrogen phosphate (KH_2PO_4). Salts were purchased from Merck Sigma-Aldrich (Saint Louis, MO, USA). Thioflavin T (ThT) dye and 2,2-Diphenyl-1-picrylhhydrazyl (DPPH) were purchased in TCI Europe (Haven, Beligum). A Büchi R-215V Rotavapor was used for solvent evaporation during NPs preparation. For dynamic light scattering (DLS) measurements an LS instrument equipped with a He-Ne laser (633 nm) was employed. Zeta potential (ZP) measurements were carried out in a Zetasizer NanoZS instrument equipped with a He-Ne laser (633 nm). For FA quantification a Breeze™2 HPLC equipped with a Symmetry® C18 5µm 4'6 x 75 mm analytical column, UV/Visible detector Waters 2489 set at 371 nm (the maximum absorption of FA), autosampler waters 2707 and binary HPLC pump waters 1525 was used. Absorbance and fluorescence measurements were conducted with a SpectraMax M5 spectrophotometer. Hyperspectral images were obtained by a Cytoviva Hyperspectral Microscope.

5.2. PREPARATION OF POLYMERIC NANO-EMULSIONS

Polymeric non-loaded nano-emulsions were prepared using the PIC low energy method. A composition of 90% phosphate-buffered saline solution (PBS), 7% oil and 3% surfactant was chosen as previous works described[1] its good compromise with a small droplet size and minimum

amount of the Food and Drugs Administration (FDA) approved T-80 surfactant (slightly irritant and harmful by inhalation).

For the preparation of a 4 ml batch of NPs, 120 µl of T-80 surfactant were firstly introduced in a test tube. Simultaneously 10 mg of PLGA measured in an analytical balance were dissolved in 280 µl of ethyl acetate. This solution was then added to the surfactant and stirred until a homogeneous and transparent mixture was obtained.

Under steady stirring at constant temperature 3.6 ml of PBS solution were added dropwise with a syringe into the surfactant, ethyl acetate and PLGA mixture solution previously prepared. As PBS was incorporated, the sample took a whitish turbid appearance. Towards the end of the PBS addition the sample turned almost transparent with a slight bluish glow.

High turbidity by the end of PBS addition indicated an improper nano-emulsion preparation with high polydispersity and large hydrodynamic diameter, therefore it was extremely important that PBS's incorporation was slow, steady and under constant stirring to obtain proper-sized NPs and avoid creaming and sedimentation[1].

Drug-loaded nano emulsions were prepared using the same procedure, but FA was added to the organic phase (ethyl acetate) at different concentrations.

5.3. PREPARATION OF POLYMERIC NPS FROM NANO-EMULSIONS

NPs were prepared from nano-emulsions by solvent evaporation under reduced pressure at 25ºC using a rotavapor. The evaporation conditions for 4 mL of nano-emulsion were: vacuum of 43 mbars and rotation speed of 150 rpm for 1 hour.

After the evaporation step, volume was adjusted with MiliQ water to maintain the osmolality of the sample around 300 mOsm/kg.

5.4. PHYSICOCHEMICAL CHARACTERIZATION OF NPS

Average droplet size distribution and polydispersity of NPs was determined by Dynamic Light Scattering (DLS) and the method of cumulants. Samples of 200 µl were evaluated using 3D cross correlation multiple scattering, scattering angle of 90º and 25ºC.

Polydispersity of the sample was assessed via the polydispersity index (PDI), calculated by the mean width value of the distribution of sizes divided by the mean value of the hydrodynamic radius[10].

The surface charge (Zeta potential, ZP) of the nanoparticles was evaluated by electrophoretic mobility measurements. Using the Smoluchowski approximation of Henry's equation[11] ZP (ζ) was calculated from electrophoretic mobility (μ_e) (Equation 1). Due to salinity of the samples, for ZP measurements 50 µl of the NPs had to be diluted to a 1 ml final volume with deionized water to avoid saturation.

$$\zeta = \frac{\mu_e \eta}{\varepsilon_r \varepsilon_0}$$

Equation 1. Smoluchowski approximation of Henry's equation. ε_r = relative permittivity/dielectric constant, ε_0= permittivity of vacuum, ζ = zeta potential, η = viscosity at experimental temperature and μ_e=electrophoretic mobility.

Data shown in the results section exhibit mean values of size, PDI and ZP drawn from triplicate measurements of each sample.

5.5. FA QUANTIFICATION ASSAYS

For FA quantification a gradient mode reversed phase chromatography (RPC) method was employed (Table 1). Mobile phases used were a 0.001 % acetic acid solution in MilliQ water (solvent A) and acetonitrile (solvent B) at 25ºC. Measures were conducted at a flow rate of 1 ml/min, injecting volume of 30 µl, and 20 min chromatogram plotting.

Time (min)	%A	%B
0	100	0
6	90	10
8	70	30
10	60	40
15	100	0

Table 1. Gradient mode for FA quantification.

5.6. ENCAPSULATION EFFICIENCY

Efficiency of FA encapsulation was evaluated by centrifugation. Centrifugal filter units with a molecular weight cut-off (MWCO) of 3 KDa were used. The centrifugation was carried out on 1 ml drug-loaded NPs during 40 min at 4ºC and 6000 rpm.

A calibration curve was built by consecutive HPLC measurements of samples with concentrations ranging from 0.5 to 0.02 FA mg/mL prepared from a 5 mg/ml stock solution of FA. Encapsulation efficiency (EE%) percentage values were determined by interpolation in the mentioned calibration curve.

5.7. HYPERSPECTRAL MICROSCOPY

Mobile Hyperspectral images were obtained using a CytoViva Hyperspectral Microscope, a technology specifically developed for spectral characterization and spectral mapping of nanoscale samples.

FA and PLGA were initially scanned to obtain hyperspectral reference images. Then, to confirm FA's encapsulation, 5 µL of the FA-loaded NPs ([FA]=0.1 mg/ml) were scanned and resulting images were compared with the references previously stored.

5.8. DRUG RELEASE EXPERIMENT

Release of FA was studied for different system conditions using the dialysis bag method. Experiments were performed at 37ºC using a cellulose membrane with a MWCO of 3000 kDa. Firstly, the membrane was pre wetted with a receptor solution for 20 minutes and then filled with 1.3 ml of the sample. Dialysis bags were immersed in the receptor solution and maintained at constant temperature with steady stirring.

Aliquots of 1 ml of the receptor solution were withdrawn at controlled intervals of time and FA concentration determined by HPLC as described in Section 5.5. After each removal step, volume was adjusted with 1 ml of the receptor solution to maintain the osmolality of the sample.

Initially, experiments were performed using PBS as the receptor solution, however, because of FA's low solubility in water, the receptor solution was replaced with a PBS/Ethanol (50/50) mixture to enhance FA's solubility. Other receptor solution conditions were also evaluated such as pH= 3 PBS/orthophosphoric acid.

Release studies were carried out in triplicate with both free FA solutions and FA-loaded NPs ([FA]=0.1 mg/ml) using a PBS/Ethanol (50/50) mixture as the receptor solution to maintain sink conditions.

5.9. *IN VITRO* STUDIES

5.9.1. DPPH assay

Radical scavenging activities of free FA and FA-loaded NPs were evaluated using the 2,2-diphenyl-1-picrylhydrazyl (DPPH) assay. FA antioxidant activity study was performed following two methods found in literature. Assays were carried out in triplicate.

Paka's method[12] was followed. Ethanolic solutions of FA-loaded NPs (0.233 and 0.112 PLGA mg/ml) were prepared. Two hundred microliters of a 0.2 mM DPPH solution in ethanol were mixed with 20 µl of the solution to be tested and introduced in a 96-well plate. Reaction mixture was incubated for 30 minutes in the darkness at room temperature.

Activity was determined by absorbance measures of the samples at 517 nm. A control sample was prepared with 20 µl ethanol and 220 µl of the 0.2 mM DPPH solution.

Measures were also performed following Piang's methodology[13]. Methanolic solutions of FA-loaded NPs (0.233 and 0.112 PLGA mg/ml) were prepared. Twenty-five ml of the solution to be tested were introduced in a 96-well plate. Then, 275 µl of a 0.004% DPPH (4 mg/100ml) in methanol were added. Reaction mixture was incubated for 1 hour at 37ºC and absorbance was measured at 517 nm. A control sample was prepared with 25 µl of methanol in 275 µl of the DPPH solution.

5.9.2. $A\beta_{1-42}$ peptide inhibition

$A\beta_{1-42}$ peptide inhibition in the presence of FA was assessed by the ThioflavinT (ThT) assay[2]. A 4.5 mg $A\beta_{1-42}$ peptide/ml solution in 1,1,1,3,3,3-hexafluoro-2-propanol (HFIP) was prepared and sonicated for 1 minute. HFIP was evaporated using a N_2 flow and traces left in the sample were eliminated by storage in vacuum followed by an overnight stay in the freezer.

The $A\beta_{1-42}$ peptide soluble aggregate generated was then dissolved in dimethyl sulfoxide (DMSO) until a 4.5 mg $A\beta_{1-42}$ peptide/ml concentration was achieved. Solutions to be tested were

introduced in a microplate and mixed with a ThT solution in PBS to a final concentration of 6.3 ThT µg/ml. The final volume of the sample in each well ought to be 200 µl. Assays were performed in duplicate.

The fluorescence emission spectrum of ThT ($\lambda_{excitation}$= 400 nm, $\lambda_{emission}$= 480 nm) was recorded after incubated alone, in presence of $A\beta_{1-42}$ peptide and with $A\beta_{1-42}$ peptide and FA-loaded NPs for 30 hours at 37ºC.

5.9.3. MTT assay

Cell viability was assessed via the 3-(4,5-dimethylthiazol-2-yl)-2,5-diphenyltetrazolium bromide (MTT) colorimetric assay. HeLa cells were seeded (about 5-6·10^3 cells per well) on a 96-well plate in Gibco Dulbecco's Modified Eagle Medium (DMEM) + 10% foetal bovine serum (FBS) and cultured for 24h at 37ºC under 5% CO_2 atmosphere.

Culture medium was next replaced and FA-loaded NPs were added at concentrations of 0.233 and 0.112 PLGA mg/ml. NPs were incubated for 24h and culture medium (100 µl) was again restocked to avoid cellular stress.

Further overnight incubation of the mixture was followed by 15 µl addition of [MTT]= 5 mg/ml solution onto the 96-well plate. After 3h, the culture medium was withdrawn carefully so as not to disengage the cells in the plate, and 100 µl of DMSO were added.

The plate was shaken for 15 min at room temperature and absorbance was measured at λ=570 nm with the spectrophotometer. Measures were carried out in duplicate of 16 wells each, for every FA-loaded NPs' concentration.

6. RESULTS AND DISCUSSIONS

6.1. PREPARATION OF POLYMERIC NPS

Polymeric nano-emulsions (non-loaded and FA-loaded) were prepared using the PIC method as described in sections 5.2 and 5.3 by steady addition of PBS to a mixture of 4% PLGA in ethyl acetate and surfactant (T-80) under constant vortexing at 25ºC and further evaporation at reduced pressures.

Formation of O/W nano-emulsion was assessed visually: samples with transparent, translucent, or slight opaque aspect, having a slight bluish shine were considered adequate.

As FA's concentration in the PLGA NPs was increased, the turbidity of the sample was noticed to augment due to increased diameter of the NPs (Figure 6).

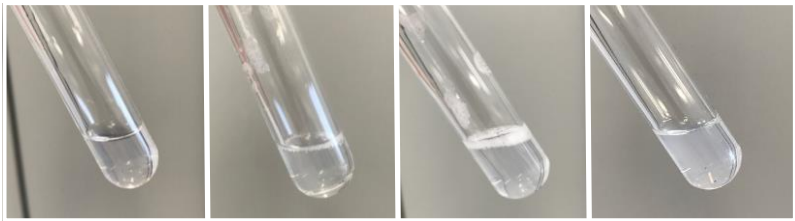

Figure 6. From left to right: i) non-loaded NPs, ii) [FA]= 0.1 mg/ml loaded NPs, iii) [FA]= 0.2 mg/ml loaded NPs, iv) [FA]= 0.3 mg/ml loaded NPs.

6.2. OPTIMISATION OF FA-LOADED NPS FORMULATION

Batches of 4 ml NPs were prepared to study the methodology's reproducibility. Nonetheless, smaller batches of 1 and 2 ml were mostly used due to its faster preparation and the need for fresh NPs for experimental procedures.

Initially, different FA concentrations were studied to determine the optimal encapsulation concentration that displayed optimal size and surface charge values with low variability. FA-

loaded NPs with FA concentrations of 0.1, 0.2 and 0.3 mg/ml were prepared. Loaded and non-loaded NPs were both characterized via DLS and ZP measurements (Table 2 and Appendix 1).

FA-loaded NPs with 0.1 mg FA/ml displayed a mean hydrodynamic diameter of 63±5 nm and a PDI of 0.25±0.08. ZP measurements showed similar negative surface charge values around -27±1 mV mainly due to the carboxylic group (COO^-) of PLGA, located on the NPs' surface.

FA-loaded NPs with 0.1 mg FA/ml displayed great reproducibility and very low variabilities. Other FA concentrations exhibited higher variability and were decided to be less adequate for further experimental studies (Table 2).

NPs-[FA] (mg/ml)	D (nm)	PDI	ZP (mV)
Non-loaded	47±5	0.27±0.03	-
0.1	63±5	0.25±0.08	-27±1
0.2	97±11	0.28±0.06	-36±3
0.3	95±28	0.35±0.03	-41±4

Table 2. Mean values of DLS and ZP measurements for FA-loaded and non-loaded NPs.

As expected, the hydrodynamic diameter increased when FA was encapsulated. An increment in FA's concentration in the NPs also induced larger diameters, although samples with 0.2 and 0.3 mg FA/ml concentrations showed very similar values. Polydispersity remained under the threshold of 0.4 and was accordingly considered acceptable.

For the ZP measurements, a gradual decrease in the surface charge was noticed. This increase in the negative zeta potential indicated high stability of the colloidal system. If all the particles in suspension have a large negative or positive zeta potential, they will tend to repel each other and there will be no tendency for the nanoparticles to come together[10].

6.3. FA ENCAPSULATION EFFICIENCY

A reversed phase chromatography (RPC) method was used for FA quantification. This procedure is based on the hydrophobic binding interactions between the solute molecules in the mobile phase and the immobilised hydrophobic ligand in the stationary phase[14].

Biomolecules like FA strongly adsorb to the surface of a reversed phase matrix under aqueous conditions, but they desorb from the matrix within a very narrow window of organic modifier concentration. Hence, RPC of biomolecules tend to use gradient elution mechanisms.

For the RPC protocol a mixture of water (0.001% acetic acid solution in MilliQ) and a miscible organic solvent (acetonitrile) were used as the mobile phase. The purpose of acetonitrile was to maintain the polarity at a level low enough for the solute to dissolve in the mobile phase and yet high enough to facilitate the binding of FA with the stationary matrix.

Once FA was bound to the column matrix, it was made to dissociate from it by decreasing the polarity further by increasing the concentration of the organic solvent in the mobile phase.

Multiple protocols were attempted but the best results were obtained under gradient elution conditions and mobile phases described above. Retention time of FA for this method was around 10.5 minutes.

To determine FA's encapsulation efficiency, the centrifugation protocol described in section 5.6 was followed. A calibration line was prepared by HPLC readings of different FA solutions in KH_2PO_4/CH_3CN (1:1) with concentrations ranging from 0.5 to 0.02 FA mg/ml.

The calibration line obtained displayed a linear regression equation of y=(1.114E+09 ± 3E+06)x + (5.4E+07 ± 8E+06) and a regression coefficient of R^2= 0.9963 (Figure 7).

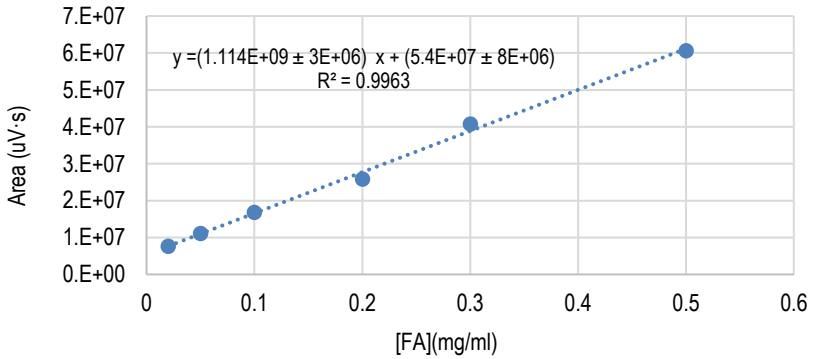

Figure 7. Calibration curve for EE% studies.

As shown in section 6.2, NPs containing [FA]=0.1 mg/ml concentration were found to display lowest variability in DLS and ZP measurements and were therefore selected for encapsulation studies.

The amount of non-loaded drug present in the supernatant liquid after centrifugation was determined by HPLC readings with the gradient elution method previously described in Table 1

and interpolation in the latter calibration curve (Figure 7). Encapsulation efficiency for [FA]=0.1 mg/ml loaded NPs was found to be 92±5% (Appendix 2).

As so to study if the concentration of FA could be increased in the NPs and still display great entrapment efficiencies, NPs containing [FA]=0.3 mg/ml were also analysed and although EE% was satisfactory (82±4%) the encapsulation efficiency for [FA]=0.1mg/ml loaded NPs was superior.

6.4. HYPERSPECTRAL SCAN

Colour mapping with intensity scaling was used to display compositional contrast between pixels in the mapping of PLGA-FA-loaded NPs.

Free FA mapping displayed a white coloration while PLGA mapping reference images appeared blue (Appendix 3). Loaded NPs images were noticed to display blue and white sections which demonstrated the correct encapsulation of FA onto the PLGA NPs.

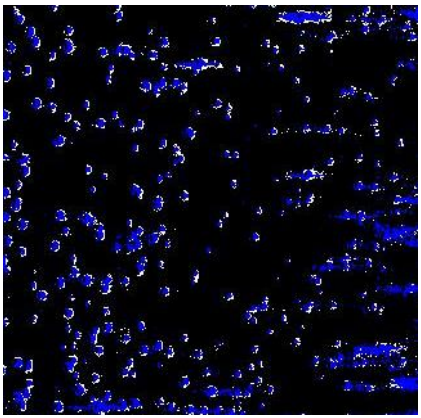

Figure 8. Mapping PLGA FA-loaded NPs ([FA]=0.1mg/ml).

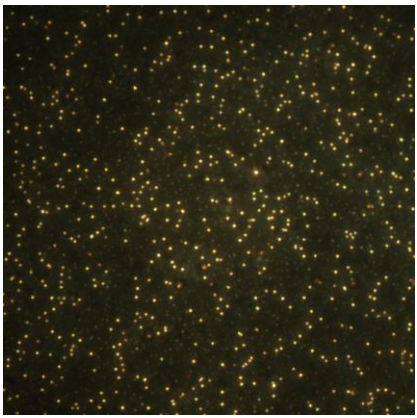

Figure 9. PLGA FA-loaded NPs 40x ([FA]=0.1mg/ml).

6.5. RELEASE STUDIES

As described in section 5.8, FA's release was studied for different system conditions using the dialysis bag method. A great number of complications were found along the experimental procedure mainly due to FA's low solubility in water.

Initial experiments were performed using PBS as the receptor solution, but FA-loaded NPs displayed extremely low FA discharge. Other receptor solution conditions were also evaluated such as a pH= 3 PBS/orthophosphoric acid solution to assess FA's dependence on pH. However, liberation percentages were still very low.

Additionally, different dialysis membrane conditions were also attempted to enhance FA's release efficiency, but values remained scarce. After much deliberation, the receptor solution was replaced with a PBS/Ethanol (50/50) mixture to enhance FA's solubility, and better release rates were observed.

Release studies were carried out in triplicate for 9 hours each for both free FA and FA-loaded NPs ([FA]=0.1 mg FA/ml). Time frame could not be prolonged any further due to ethanol's volatility at experimental conditions of 37ºC as alterations during experimental procedure would highly affect FA's liberation rates and experimental error.

The calibration curve used for encapsulation efficiency calculations could not be employed for release studies as FA's discharge concentrations were out of range. Concentration of FA was assessed via HPLC by interpolation onto the following calibration curve y=(1.12E+09 ± 2E+07)x -(4.4E+05± 3E-04) with a regression coefficient of R^2= 0.9973 (Appendix 4). Only about 5.2±0.8 of free FA was observed to be released within the 9-hour time frame, whilst FA-loaded NPs improved its liberation up to 23±3% (Figure 10 and Appendix 5).

It would be expected that free FA solutions display faster release rates as compared to encapsulated systems due to the free drug's superior mobility and ease to cross the dialysis membrane, but this was not the case for the present experiments. Other works[15] regarding FA's release have been found to exhibit similar behaviours.

FA-loaded NPs showed higher FA release, improving a sustained drug delivery. Moreover, FA encapsulation in PLGA NPs prevents FA degradation in the blood stream and could enable great permeabilities trough the BBB barrier enhancing FA's access to the brain.

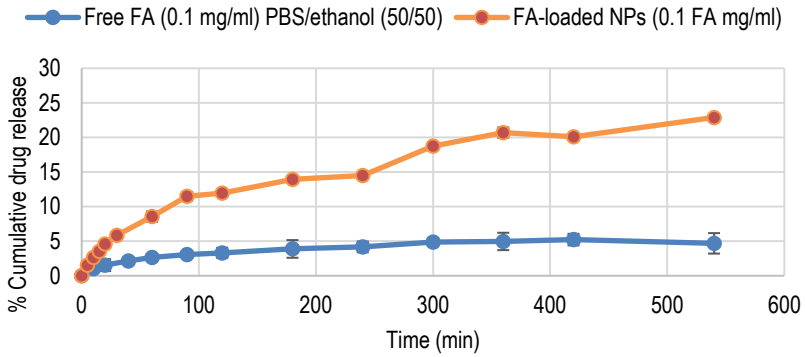

Figure 10. Mean % cumulative drug release profiles of free FA and FA-loaded NPs.

Mathematical models are an important tool to evaluate drug release processes *in vitro* and *in vivo*, design pharmaceutical formulations and determine optimal design for new systems. Various mathematical models of drug release were fitted to determine FA-loaded NPs' release profile using the Solver tool in Microsoft Excel. Among main-release kinetic models[16] fittings by Higuchi and Korsmeyer-Peppas displayed the best correlation coefficients (Table 3 and Appendix 6).

	Equation	R^2	Parameters
Korsmeyer-Peppas	$f_i = Kt^n$ f_i= amount of drug released K =release velocity constant n = exponent of release t= time	0.993	K =1.16 n = 0.48
Higuchi	$f_i = K_H\sqrt{t}$ f_i= amount of drug released K_H =release constant of Higuchi t= time	0.994	K_H =1.03

Table 3. Performed fittings for FA-loaded NPs release.

Value of the Korsmeyer-Peppas exponent of release (n) allowed to establish system's release behaviour. For 0.43<n<0.85 (for spheric polymeric matrixes) the model implies non-Fickian or anomalous transport, and the mechanism of drug release is governed by diffusion and swelling[16].

6.6. DPPH ASSAY

Radical scavenging activities of free FA and FA-loaded NPs were evaluated using the 2,2-diphenyl-1-picrylhydrazyl (DPPH) assay. The scavenging ability of FA against DPPH radical is dependent on the hydroxyl group of the benzene ring and the ortho substitution with the electron donor methoxy group, which increases the stability of the phenoxy radical[8]. FA's radical is highly stabilised due to its structure, which enables delocalization of electron density (Figure 11).

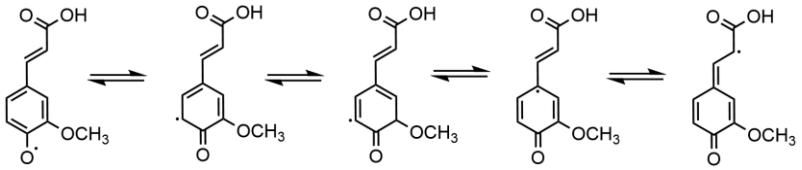

Figure 11. FA resonant structures.

During DPPH's reduction (Figure 12), radical DPPH electron is captured by FA's hydroxyl group and further delocalized in the acid's structure. Reduction of DPPH induces a change of coloration from purple to yellow. DPPH reduction was assessed visually and by absorbance measurements using a spectrophotometer.

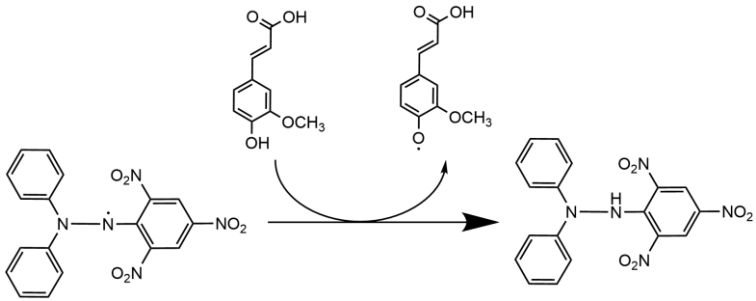

Figure 12. DPPH reduction in FA's presence.

Previous *in vitro* studies determined that 0.233 and 0.112 PLGA mg/ml concentrations displayed non-toxic behaviours. NPs containing [FA]=0.1 mg/ml and [FA]=0.2 mg/ml were used to prepare solutions of PLGA concentrations mentioned above for experimental procedure.

From the two methods found in literature, Paka's procedure exhibited less variableness and better inhibition rates, so only results following this method are shown in this work. Higher concentrations of FA displayed higher inhibition rates of the DPPH radical (Figure 13 and Table 4) confirming radical scavenging properties of FA and therefore its potential as a therapeutic agent for AD treatment.

	Inhibition rate (%)			
Samples	1	2	3	$\bar{x}_{inhibition}$
[FA]= 0.004 mg/ml [PLGA]=0.112 mg/ml	20.49	20.51	17.34	19 ± 2
[FA]= 0.008 mg/ml [PLGA]=0.112 mg/ml	27.66	28.36	25.24	27 ± 2
[FA]= 0.02 mg/ml [PLGA]=0.233 mg/ml	49.33	43.31	36.59	43 ± 6
Free [FA]= 0.1 mg/ml	69.21	74.04	71.32	72 ± 2

Table 4. % Inhibition rates measured by Paka's method.

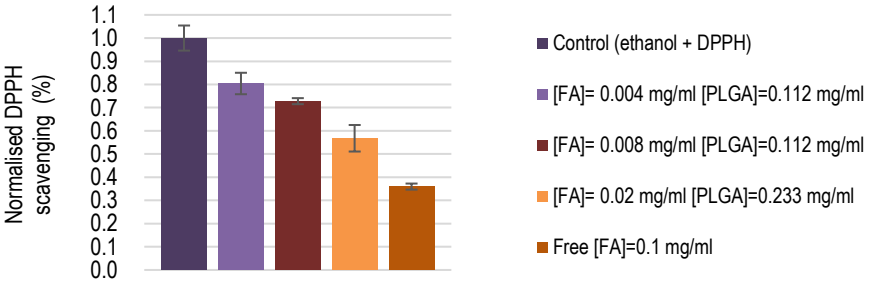

Figure 13. % Normalized inhibition rates by Paka's method.

6.7. Aβ$_{1-42}$ PEPTIDE INHIBITION

The formation of β-rich peptide self-assemblies is associated with a diverse set of the so-called protein misfolding diseases. In AD, Aβ fibril accumulation and plaque formation are thought to be one of the major causes of the disease and strategies targeting its disaggregation are key for future therapies.

Thioflavin T (ThT) is a benzothiazole dye that exhibits enhanced fluorescence upon binding to amyloid fibrils and is commonly used to diagnose protein-misfolding diseases. In 1959, Vassar and Culling demonstrated the potential of fluorescent microscopy for amyloid fibril diagnosis in a pioneering report and later in the late 1980s and early 1990s Naiki et al. and LeVine were among

the first to thoroughly characterize the fluorescence spectra and binding properties of ThT to amyloid fibrils[17].

Fibrils and other peptide self-assemblies are insoluble and often heterogeneous in their composition, making it extremely difficult to characterize their interactions with ligands and so, mechanism by which ThT recognizes and binds peptide self-assemblies remains poorly understood[17] even though electrostatic interactions are known to participate (Figure 14). Some studies have suggested enhancement of fluorescence upon binding is due to the rotational immobilization of the central C–C bond connecting the benzothiazole and aniline rings[18].

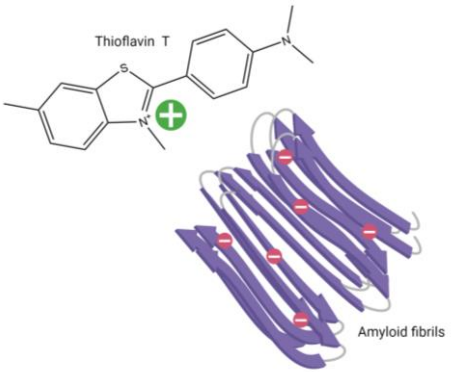

Figure 14. ThT recognition and binding to peptide self-assemblies.

$A\beta_{1-42}$ peptide inhibition was studied in this work following the ThT assay described in Section 5.9.2. After incubation of the peptide with FA-loaded NPs and ThT for 30 hours, $A\beta_{1-42}$ fibrils disaggregation was expected and consequently a decrease in fluorescence brightness. Nevertheless, fluorescence increased significantly after incubation.

Papers[3,19,20] in regard to this experimental procedure did not accurately describe addition step of ThT fluorescent dye and after a careful review of the experimental methodology it was noted that ThT should have been added after incubation.

When mixed with $A\beta_{1-42}$ fibrils ThT interactions result in strong fluorescence signals on account of the ThT's binding to the fibrils. Overtime, fluorescence ought to diminish due to FA-loaded NPs effects on $A\beta_{1-42}$ fibrils disentanglement. Nonetheless, initial binding of ThT to the

peptide self-assemblies could interfere in FA-loaded NPs' interaction with the fibrils, resulting in strong fluorescence signals after incubation.

Unfortunately, due to $A\beta_{1-42}$ peptide unavailability, further studies could not be completed. Results from this section are not shown in this work as they should be repeated and further analysed.

6.8. MTT ASSAY

This project's main purpose is to study potential applications of FA-loaded NPs as therapeutic agents for AD treatment. Consequently, performance of cell viability studies is crucial to ensure the prepared NPs display non-toxic behaviours.

PLGA is an FDA approved biocompatible polymer extensively used in delivery drug systems. Concentrations under 0.233 PLGA mg/mL have been found to be innocuous and adequate for *in vitro* studies, but FA-loaded NPs ought to be evaluated to assess cell's response to FA's encapsulation.

Cell's response to FA-loaded NPs was determined via the 3-(4,5-dimethylthiazol-2-yl)-2,5-diphenyltetrazolium bromide (MTT) colorimetric assay[21]. This methodology is based on NAD(P)H-dependent oxidoreductase enzymes, largely present in the cytosolic compartment of the cells. These enzymes can reduce the tetrazolium dye MTT to its insoluble form formazan and under defined conditions it can reflect the number of viable cells present in a sample[22]. MTT reduction to formazan (Figure 15) induces a change in coloration from yellow to purple which can be assessed by absorbance measurements in a spectrophotometer.

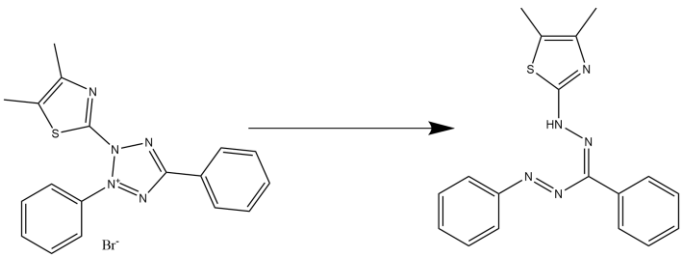

Figure 15. MTT reduction to formazan by cytosolic NAD(P)H-dependent oxidoreductase enzyme.

For this procedure [FA]=0.1 mg/ml loaded NPs were used as stock solutions for the preparation of 0.233 and 0.112 PLGA mg/ml samples.

FA-loaded NPs did not exhibit noxious effects on HeLA cells nor its proliferation after 24 h incubation and cellular viability percentages of loaded NPs displayed even lower toxicities than non-loaded PLGA NPs. Higher concentrations of PLGA did show slightly higher toxicities but absorbance measures demonstrated non-toxic response *in vitro* (Figure 16).

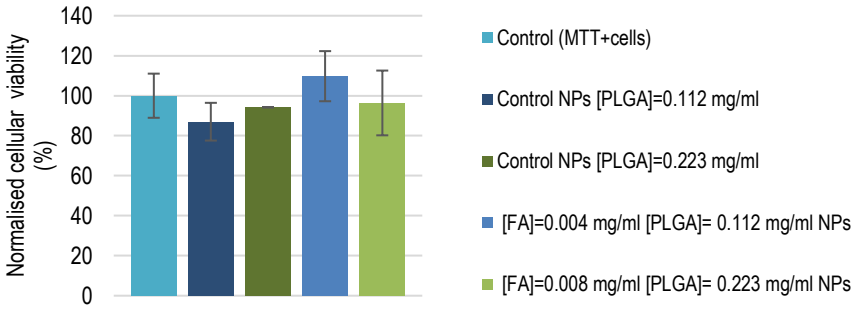

Figure 16. % Normalised cell viability by MTT assay.

10. CONCLUSIONS

In this work, FA-loaded PLGA NPs were prepared by nano-emulsion templating using the PIC method in an attempt to study the application of these nanocarriers as therapeutic systems for AD treatments. Optimisation of FA-loaded NPs formulation was assessed by DLS and ZP measurements and encapsulation efficiency was evaluated via HPLC and hyperspectral microscopy.

Release experiments demonstrated enhanced discharge rates for FA-loaded NPs versus free FA solutions. Drug-loaded NPs displayed prolonged and sustained drug liberation rates and moreover could prevent FA's degradation in the blood stream as well as increase water solubility and permeabilities through the BBB.

Further *in vitro* studies were also performed to confirm non-toxic behaviour of FA-loaded NPs in biological systems and FA's radical scavenging properties. Unfortunately, Aβ fibril disaggregation by FA-loaded PLGA NPs could not be properly assessed due to peptide's unavailability.

11. REFERENCES AND NOTES

(1) Solans, C.; Solé, I. Nano-Emulsions: Formation by Low-Energy Methods. *Curr. Opin. Colloid Interface Sci.* **2012**, *17* (5), 246–254. https://doi.org/10.1016/j.cocis.2012.07.003.

(2) Jha, A.; Ghormade, V.; Kolge, H.; Paknikar, K. M. Dual Effect of Chitosan-Based Nanoparticles on the Inhibition of β-Amyloid Peptide Aggregation and Disintegration of the Preformed Fibrils. *J. Mater. Chem. B* **2019**, *7* (21), 3362–3373. https://doi.org/10.1039/C9TB00162J.

(3) Singh, Y. P.; Rai, H.; Singh, G.; Singh, G. K.; Mishra, S.; Kumar, S.; Srikrishna, S.; Modi, G. A Review on Ferulic Acid and Analogs Based Scaffolds for the Management of Alzheimer's Disease. *Eur. J. Med. Chem.* **2021**, *215*, 113278. https://doi.org/10.1016/j.ejmech.2021.113278.

(4) O'Brien, R. J.; Wong, P. C. Amyloid Precursor Protein Processing and Alzheimer's Disease. *Annu. Rev. Neurosci.* **2011**, *34* (1), 185–204. https://doi.org/10.1146/annurev-neuro-061010-113613.

(5) Sgarbossa, A.; Giacomazza, D.; Di Carlo, M. Ferulic Acid: A Hope for Alzheimer's Disease Therapy from Plants. *Nutrients* **2015**, *7* (7), 5764–5782. https://doi.org/10.3390/nu7075246.

(6) Mori, T.; Koyama, N.; Guillot-Sestier, M.-V.; Tan, J.; Town, T. Ferulic Acid Is a Nutraceutical β-Secretase Modulator That Improves Behavioral Impairment and Alzheimer-like Pathology in Transgenic Mice. *PLoS ONE* **2013**, *8* (2), e55774. https://doi.org/10.1371/journal.pone.0055774.

(7) Inokuchi, R.; Takaichi, H.; Kawano, T. Fluorometric Quantification of Ferulic Acid Concentrations Based on Deconvolution of Intrinsic Fluorescence Spectra. *Environ. Control Biol.* **2016**, *54* (1), 57–64. https://doi.org/10.2525/ecb.54.57.

(8) Kikuzaki, H.; Hisamoto, M.; Hirose, K.; Akiyama, K.; Taniguchi, H. Antioxidant Properties of Ferulic Acid and Its Related Compounds. *J. Agric. Food Chem.* **2002**, *50* (7), 2161–2168. https://doi.org/10.1021/jf011348w.

(9) Fornaguera, C.; Dols-Perez, A.; Calderó, G.; García-Celma, M. J.; Camarasa, J.; Solans, C. PLGA Nanoparticles Prepared by Nano-Emulsion Templating Using Low-Energy Methods as Efficient Nanocarriers for Drug Delivery across the Blood–Brain Barrier. *J. Controlled Release* **2015**, *211*, 134–143. https://doi.org/10.1016/j.jconrel.2015.06.002.

(10) Bhattacharjee, S. DLS and Zeta Potential – What They Are and What They Are Not? *J. Controlled Release* **2016**, *235*, 337–351. https://doi.org/10.1016/j.jconrel.2016.06.017.

(11) Honary, S.; Zahir, F. Effect of Zeta Potential on the Properties of Nano-Drug Delivery Systems - A Review (Part 1). *Trop. J. Pharm. Res.* **2013**, *12* (2), 255–264. https://doi.org/10.4314/tjpr.v12i2.19.

(12) Djiokeng Paka, G.; Doggui, S.; Zaghmi, A.; Safar, R.; Dao, L.; Reisch, A.; Klymchenko, A.; Roullin, V. G.; Joubert, O.; Ramassamy, C. Neuronal Uptake and Neuroprotective Properties of Curcumin-Loaded Nanoparticles on SK-N-SH Cell Line: Role of Poly(Lactide- *Co* -Glycolide) Polymeric Matrix Composition. *Mol. Pharm.* **2016**, *13* (2), 391–403. https://doi.org/10.1021/acs.molpharmaceut.5b00611.

(13) Piang-Siong, W.; de Caro, P.; Marvilliers, A.; Chasseray, X.; Payet, B.; Shum Cheong Sing, A.; Illien, B. Contribution of Trans -Aconitic Acid to DPPH Scavenging Ability in Different Media. *Food Chem.* **2017**, *214*, 447–452. https://doi.org/10.1016/j.foodchem.2016.07.083.

(14) Horviith, C. Reversed-Phase Chromatography. *Trends Anal. Chem.* **1981**, 7.

(15) Saini, S.; Sharma, T.; Jain, A.; Kaur, H.; Katare, O. P.; Singh, B. Systematically Designed Chitosan-Coated Solid Lipid Nanoparticles of Ferulic Acid for Effective Management of Alzheimer's Disease: A Preclinical Evidence. *Colloids Surf. B Biointerfaces* **2021**, *205*, 111838. https://doi.org/10.1016/j.colsurfb.2021.111838.

(16) Mathematical Models of Drug Release. In *Strategies to Modify the Drug Release from Pharmaceutical Systems*; Elsevier, 2015; pp 63–86. https://doi.org/10.1016/B978-0-08-100092-2.00005-9.
(17) Biancalana, M.; Makabe, K.; Koide, A.; Koide, S. Molecular Mechanism of Thioflavin-T Binding to the Surface of β-Rich Peptide Self-Assemblies. *J. Mol. Biol.* **2009**, *385* (4), 1052–1063. https://doi.org/10.1016/j.jmb.2008.11.006.
(18) Xue, C.; Lin, T. Y.; Chang, D.; Guo, Z. Thioflavin T as an Amyloid Dye: Fibril Quantification, Optimal Concentration and Effect on Aggregation. *R. Soc. Open Sci.* **2017**, *4* (1), 160696. https://doi.org/10.1098/rsos.160696.
(19) Liu, Y.; Liu, Y.; Wang, S.; Dong, S.; Chang, P.; Jiang, Z. Structural Characteristics of (−)-Epigallocatechin-3-Gallate Inhibiting Amyloid Aβ42 Aggregation and Remodeling Amyloid Fibers. *RSC Adv.* **2015**, *5* (77), 62402–62413. https://doi.org/10.1039/C5RA09608A.
(20) Baysal, I.; Ucar, G.; Gultekinoglu, M.; Ulubayram, K.; Yabanoglu-Ciftci, S. Donepezil Loaded PLGA-b-PEG Nanoparticles: Their Ability to Induce Destabilization of Amyloid Fibrils and to Cross Blood Brain Barrier in Vitro. *J. Neural Transm.* **2017**, *124* (1), 33–45. https://doi.org/10.1007/s00702-016-1527-4.
(21) David M. L. Morgan. *Tetrazolium (MTT) Assay for Cellular Viability and Activity*.
(22) Mosmann, T. Rapid Colorimetric Assay for Cellular Growth and Survival: Application to Proliferation and Cytotoxicity Assays. *J. Immunol. Methods* **1983**, *65* (1–2), 55–63. https://doi.org/10.1016/0022-1759(83)90303-4.

12. ACRONYMS

AD Alzheimer's disease

APP Amyloid precursor protein

Aβ Beta-amyloid protein

BBB Blood-brain barrier

DLS Dynamic Light Scattering

DMEM Gibco Dulbecco's Modified Eagle Medium

DPPH 2,2-diphenyl-1-picrylhydrazyl

FA Ferulic acid

FBS Foetal bovine serum

FDA Food and drug administration

HPLC High performance liquid chromatography

MTDL Multi-target directed ligand

MTT 3-(4,5-dimethylthiazol-2-yl)-2,5-diphenyltetrazolium bromide

NCD non-communicable disease

PBS Phosphate buffered saline

PIC Phase inversion composition

PLG Poly(D,L-glycolic acid)

PLA Polylactic acid polymer

PLGA Poly(lactic-co-glycolic acid)

ROS Reactive oxygen species

Th T Thioflavin T

T-80 Polyoxyethylene polysorbate 80 or Tween 80

rpm Revolutions per minute

UV-vis Ultraviolet-visible spectroscopy

ZP Zeta potential

APPENDICES

APPENDIX 1: DLS AND ZP MEASUREMENTS

Batch	D (nm)	PDI
	47.0	0.27
1	47.3	0.29
	45.5	0.31
	45.7	0.23
2	43.2	0.28
	56.3	0.34

Table A1. DLS measurements of non-loaded PLGA NPs.

Batch	D (nm)	PDI	ZP (mV)
	58.9	0.23	-25.4
1	61.9	0.30	-26.9
	59.5	0.28	-25.3
	56.8	0.40	-26.0
2	59.5	0.38	-25.4
	60.1	0.43	-25.1
	70.7	0.26	-24.9
3	69.4	0.15	-27.1
	66.6	0.32	-25.1
	64.5	0.34	-24.6
4	55.5	0.43	-27.6
	53.8	0.38	-27.7
	54.6	0.37	-27.9
5	60.2	0.34	-26.5
	67.9	0.42	-27.3
	70.6	0.35	-25.4
6	69.9	0.24	-28.9
	67.8	0.23	-27.3
	67.6	0.25	-26.6
7	62.0	0.23	-28.4
	66.5	0.26	-27.3

Table A1. DLS and ZP measurements of loaded [FA]= 0.1 mg/ml PLGA NPs.

Batch	D (nm)	PDI	ZP (mV)
	107.2	0.34	-34.5
1	103.3	0.38	-39.0
	110.7	0.40	-37.6
	87.3	0.35	-35.5
2	88.0	0.33	-39.1
	86.1	0.35	-32.4

Table A3. DLS and ZP measurements of loaded [FA]= 0.2 mg/ml PLGA NPs.

Batch	D (nm)	PDI
	137.0	0.26
1	134.7	0.33
	134.5	0.31
	98.9	0.15
2	111.3	0.20
	106.3	0.24
	105.7	0.31
3	70.8	0.27
	71.3	0.31
	71.2	0.41
4	80.2	0.31
	59.0	0.29

Table A4. DLS measurements of loaded [FA]= 0.3 mg/ml PLGA NPs.

APPENDIX 2: FA ENCAPSULATION EFFICIENCY

NP_S [FA](mg/ml)	Area (uV·s)	[FA](mg/ml)	Dilution factor	$[FA]_{real}$ (mg/ml)	%EE
0.1	8643486	3.64E-02	0.40	1.46E-02	85.43
0.1	8169930	3.17E-02	0.40	1.27E-02	87.32
0.1	5480165	4.80E-03	0.50	2.40E-03	97.60
0.1	6054514	10.5E-02	0.50	5.27E-03	94.73
0.1	5972433	9.72E-03	0.50	4.86E-03	95.14

Table A5. Encapsulation efficiency for [FA]= 0.1 mg/ml loaded NPs.

NP_S [FA](mg/ml)	Area (uV·s)	[FA](mg/ml)	Dilution factor	$[FA]_{real}$ (mg/ml)	%EE
0.3	11315537	7.30E-02	0.56	4.10E-02	86.45
0.3	13187418	9.20E-02	0.60	5.50E-02	81.63
0.3	13594587	9.60E-02	0.70	6.80E-02	77.47
0.3	13707755	9.70E-02	0.56	5.40E-02	82.02

Table A6. Encapsulation efficiency for [FA]= 0.3 mg/ml loaded NPs.

APPENDIX 3: HYPERSPECTRAL MICROSCOPY IMAGES

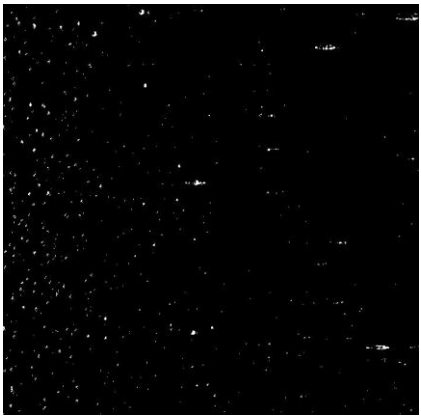

Figure A1. Mapping of FA.

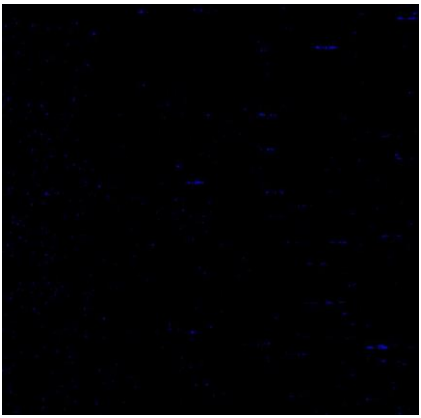

Figure A2. Mapping of PLGA.

APPENDIX 4: CALIBRATION CURVE FOR RELEASE STUDIES

[FA] (mg/ml)	Area (uV·s)
0.00024375	20572
0.0004875	44829
0.000975	89031
0.00195	207081
0.0039	396443
0.0078	754354
0.0156	1608497
0.0312	3555591

Table A7. Calibration curve data.

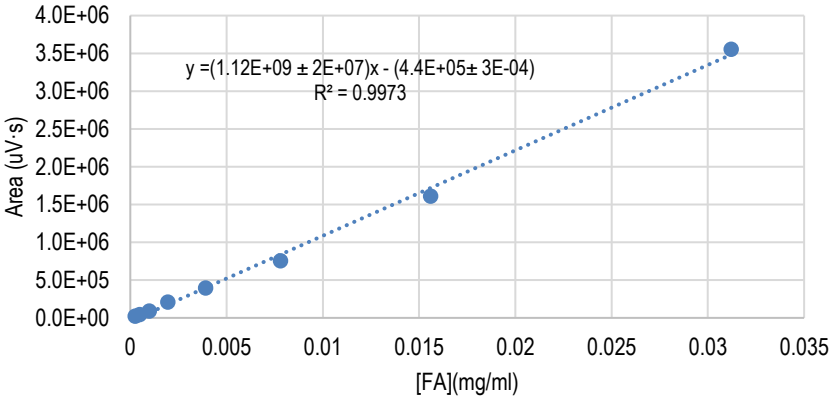

Figure A3. Calibration curve.

APPENDIX 5: RELEASE EXPERIMENTAL DATA

Time (min)	% Release
0	0
10	1.0±0.2
20	1.5±0.1
40	2.1±0.5
60	2.66±0.09
90	3.1±0.3
120	3.3±0.7
180	3.9±0.6
240	4.2±0.4
300	4.9±0.5
360	5.0±0.3
420	5.2±0.8
540	4.7±0.7

Table A8. Free FA release.

Time (min)	% Release
0	0
5	1.53±0.09
10	2.7±0.8
15	3.5±0.5
20	4.6±0.4
30	5.8±0.2
60	8.6±0.7
90	11±1
120	11.9±0.8
180	13.9±0.6
240	14±1
300	18.8±0.8
360	21±1
420	20±2
540	23±3

Table A9. FA-loaded NPs ([FA]=0.1 mg/ml) release.

Time (min)	Area (uV·s)	Conc. Extrapolada (mg/ml)	Receptor solution volume (ml)	Removed volume (ml)	Inst. Amnt (mg)	Lost Amnt (mg)	Cumul. Amnt (mg)	Real FA conc. (mg/ml)	% Release
0	0	0	30	1	0	0	0	0	0
10	57932	1.01E-03	30	1	3.04E-02	1.01E-03	3.04E-02	1.01E-03	1.0
20	123986	1.67E-03	30	1	5.02E-02	1.67E-03	5.13E-02	1.71E-03	1.7
40	208151	2.52E-03	30	1	7.55E-02	2.52E-03	7.82E-02	2.61E-03	2.6
60	208151	2.52E-03	30	1	7.55E-02	2.52E-03	8.07E-02	2.69E-03	2.7
90	226378	2.70E-03	30	1	8.10E-02	2.70E-03	8.87E-02	2.96E-03	3.0
120	205203	2.49E-03	30	1	7.46E-02	2.49E-03	8.50E-02	2.83E-03	2.8
180	280599	3.24E-03	30	1	9.72E-02	3.24E-03	1.10E-01	3.67E-03	3.7
240	301104	3.45E-03	30	1	1.03E-01	3.45E-03	1.20E-01	3.98E-03	4.0
300	396708	4.40E-03	30	1	1.32E-01	4.40E-03	1.52E-01	5.06E-03	5.1
360	339882	3.83E-03	30	1	1.15E-01	3.83E-03	1.39E-01	4.63E-03	4.6
420	345648	3.89E-03	30	1	1.17E-01	3.89E-03	1.45E-01	4.82E-03	4.8
540	276453	3.20E-03	30	1	9.60E-02	3.20E-03	1.28E-01	4.26E-03	4.3

Table A10. Control 1: Free [FA]= 0.1 mg/ml.

Time (min)	Area (uV·s)	Conc. Extrapolada (mg/ml)	Receptor solution volume (ml)	Removed volume (ml)	Inst. Amnt (mg)	Lost Amnt (mg)	Cumul. Amnt (mg)	Real FA conc. (mg/ml)	% Release
0	0	0	30	1	0	0	0	0	0
10	42826	8.63E-04	30	1	2.59E-02	8.63E-04	2.59E-02	8.63E-04	0.9
20	98062	1.42E-03	30	1	4.25E-02	1.42E-03	4.33E-02	1.44E-03	1.4
40	165468	2.09E-03	30	1	6.27E-02	2.09E-03	6.50E-02	2.17E-03	2.2
60	214966	2.58E-03	30	1	7.75E-02	2.58E-03	8.19E-02	2.73E-03	2.7
90	277299	3.21E-03	30	1	9.62E-02	3.21E-03	1.03E-01	3.44E-03	3.4
120	221810	2.65E-03	30	1	7.96E-02	2.65E-03	1.25E-01	4.16E-03	4.2
180	254823	2.98E-03	30	1	8.95E-02	2.98E-03	1.37E-01	4.57E-03	4.6
240	249721	2.93E-03	30	1	8.80E-02	2.93E-03	1.39E-01	4.62E-03	4.6
300	300055	3.44E-03	30	1	1.03E-01	3.44E-03	1.57E-01	5.22E-03	5.2
360	298765	3.42E-03	30	1	1.03E-01	3.42E-03	1.60E-01	5.33E-03	5.3
420	344526	3.88E-03	30	1	1.16E-01	3.88E-03	1.77E-01	5.90E-03	5.9
540	295634	3.39E-03	30	1	1.02E-01	3.39E-03	1.66E-01	5.54E-03	5.5

Table A11. Control 2: Free [FA]= 0.1 mg/ml .

Time (min)	Area (uV·s)	Conc. Extrapolada (mg/ml)	Receptor solution volume (ml)	Removed volume (ml)	Inst. Amnt (mg)	Lost Amnt (mg)	Cumul. Amnt (mg)	Real FA conc. (mg/ml)	% Release
0	0	0	30	1	0	0	0	0	0
10	78966	1.22E-03	30	1	3.67E-02	1.22E-03	3.67E-02	1.22E-03	1.2
20	98672	1.42E-03	30	1	4.27E-02	1.42E-03	4.39E-02	1.46E-03	1.5
40	112984	1.56E-03	30	1	4.69E-02	1.56E-03	4.96E-02	1.65E-03	1.7
60	197663	2.41E-03	30	1	7.23E-02	2.41E-03	7.66E-02	2.55E-03	2.6
90	219847	2.63E-03	30	1	7.90E-02	2.63E-03	8.56E-02	2.85E-03	2.9
120	223546	2.67E-03	30	1	8.01E-02	2.67E-03	8.94E-02	2.98E-03	3.0
180	256766	3.00E-03	30	1	9.01E-02	3.00E-03	1.02E-01	3.40E-03	3.4
240	299199	3.43E-03	30	1	1.03E-01	3.43E-03	1.18E-01	3.92E-03	3.9
300	330982	3.74E-03	30	1	1.12E-01	3.74E-03	1.31E-01	4.36E-03	4.4
360	376592	4.20E-03	30	1	1.26E-01	4.20E-03	1.48E-01	4.94E-03	4.9
420	366574	4.10E-03	30	1	1.23E-01	4.10E-03	1.49E-01	4.98E-03	5.0
540	281743	3.25E-03	30	1	9.76E-02	3.25E-03	1.28E-01	4.27E-03	4.3

Table A12. Control 3: Free [FA]= 0.1 mg/ml.

Time (min)	Area (uV·s)	Conc. Extrapolada (mg/ml)	Receptor solution volume (ml)	Removed volume (ml)	Inst. Amnt (mg)	Lost Amnt (mg)	Cumul. Amnt (mg)	Real FA conc. (mg/ml)	% Release
0	0	0	30	1	0	0	0	0	0
5	98768	1.42E-03	30	1	4.27E-02	1.42E-03	4.27E-02	1.42E-03	1.4
10	123876	1.67E-03	30	1	5.02E-02	1.67E-03	5.16E-02	1.72E-03	1.7
15	243566	2.87E-03	30	1	8.61E-02	2.87E-03	8.92E-02	2.97E-03	3.0
20	345611	3.89E-03	30	1	1.17E-01	3.89E-03	1.23E-01	4.09E-03	4.1
30	487654	5.31E-03	30	1	1.59E-01	5.31E-03	1.69E-01	5.64E-03	5.6
60	678567	7.22E-03	30	1	2.17E-01	7.22E-03	2.32E-01	7.73E-03	7.7
90	1034520	1.08E-02	30	1	3.23E-01	1.08E-02	3.46E-01	1.15E-02	11.5
120	1129894	1.17E-02	30	1	3.52E-01	1.17E-02	3.85E-01	1.28E-02	12.8
180	1243568	1.29E-02	30	1	3.86E-01	1.29E-02	4.31E-01	1.44E-02	14.4
240	1132456	1.18E-02	30	1	3.53E-01	1.18E-02	4.11E-01	1.37E-02	13.7
300	1678993	1.72E-02	30	1	5.17E-01	1.72E-02	5.86E-01	1.95E-02	19.5
360	1895643	1.94E-02	30	1	5.82E-01	1.94E-02	6.69E-01	2.23E-02	22.3
420	1798990	1.84E-02	30	1	5.53E-01	1.84E-02	6.59E-01	2.20E-02	22.0
540	2177659	2.22E-02	30	1	6.66E-01	2.22E-02	7.91E-01	2.64E-02	26.4

Table A13. Replicate 1: [FA]= 0.1 mg/ml loaded NPs.

Time (min)	Area (uV·s)	Conc. Extrapolada (mg/ml)	Receptor solution volume (ml)	Removed volume (ml)	Inst. Amnt (mg)	Lost Amnt (mg)	Cumul. Amnt (mg)	Real FA conc. (mg/ml)	% Release
0	0	0	30	1	0	0	0	0	0
5	116291	1.60E-03	30	1	4.79E-02	1.60E-03	4.79E-02	1.60E-03	16
10	240162	2.84E-03	30	1	8.51E-02	2.84E-03	8.67E-02	2.89E-03	2.9
15	317650	3.61E-03	30	1	1.08E-01	3.61E-03	1.13E-01	3.76E-03	3.8
20	423366	4.67E-03	30	1	1.40E-01	4.67E-03	1.48E-01	4.94E-03	4.9
30	510240	5.54E-03	30	1	1.66E-01	5.54E-03	1.79E-01	5.96E-03	6.0
60	801223	8.45E-03	30	1	2.53E-01	8.45E-03	2.72E-01	9.06E-03	9.1
90	887938	9.31E-03	30	1	2.79E-01	9.31E-03	3.06E-01	1.02E-02	10.2
120	994143	1.04E-02	30	1	3.11E-01	1.04E-02	3.47E-01	1.16E-02	11.6
180	1126757	1.17E-02	30	1	3.51E-01	1.17E-02	3.97E-01	1.32E-02	13.2
240	1152793	1.20E-02	30	1	3.59E-01	1.20E-02	4.17E-01	1.39E-02	13.9
300	1606055	1.65E-02	30	1	4.95E-01	1.65E-02	5.65E-01	1.88E-02	18.8
360	1717790	1.76E-02	30	1	5.28E-01	1.76E-02	6.15E-01	2.05E-02	20.5
420	1504102	1.55E-02	30	1	4.64E-01	1.55E-02	5.68E-01	1.89E-02	18.9
540	1608383	1.65E-02	30	1	4.96E-01	1.65E-02	6.15E-01	2.05E-02	20.5

Table A14. Replicate 2: [FA]= 0.1 mg/ml loaded NPs.

Time (min)	Area (uV·s)	Conc. Extrapolada (mg/ml)	Receptor solution volume (ml)	Removed volume (ml)	Inst. Amnt (mg)	Lost Amnt (mg)	Cumul. Amnt (mg)	Real FA conc. (mg/ml)	% Release
0	0	0	30	1	0	0	0	0	0
5	112907	1.56E-03	30	1	4.69E-02	1.56E-03	4.69E-02	1.56E-03	1.6
10	291907	3.35E-03	30	1	1.01E-01	3.35E-03	1.02E-01	3.41E-03	3.4
15	328581	3.72E-03	30	1	1.12E-01	3.72E-03	1.17E-01	3.88E-03	3.9
20	398981	4.42E-03	30	1	1.33E-01	4.42E-03	1.41E-01	4.71E-03	4.7
30	505367	5.49E-03	30	1	1.65E-01	5.49E-03	1.78E-01	5.92E-03	5.9
60	786440	8.30E-03	30	1	2.49E-01	8.30E-03	2.68E-01	8.92E-03	8.9
90	1143076	1.19E-02	30	1	3.56E-01	1.19E-02	3.83E-01	1.28E-02	12.8
120	968117	1.01E-02	30	1	3.03E-01	1.01E-02	3.42E-01	1.14E-02	11.4
180	1027159	1.07E-02	30	1	3.21E-01	1.07E-02	4.25E-01	1.42E-02	14.2
240	1240067	1.28E-02	30	1	3.85E-01	1.28E-02	4.79E-01	1.60E-02	16.0
300	1467864	1.51E-02	30	1	4.53E-01	1.51E-02	5.36E-01	1.79E-02	17.9
360	1657354	1.70E-02	30	1	5.10E-01	1.70E-02	5.80E-01	1.93E-02	19.3
420	1706518	1.75E-02	30	1	5.25E-01	1.75E-02	5.80E-01	1.93E-02	19.3
540	2008211	2.05E-02	30	1	6.16E-01	2.05E-02	6.54E-01	2.18E-02	21.8

Table A15. Replicate 3: [FA]= 0.1 mg/ml loaded NPs.

APPENDIX 6: RELEASE FITTINGS

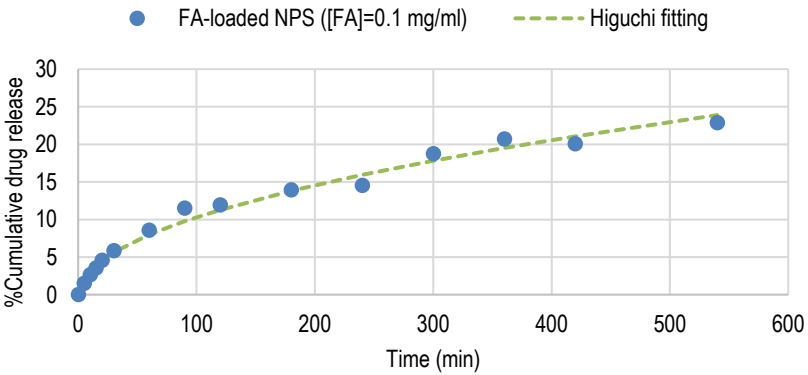

Figure A4. Higuchi fitting for the release of FA-loaded NPs.

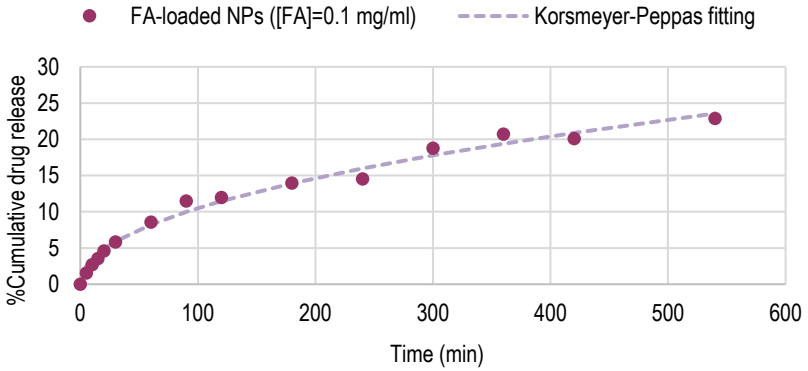

Figure A5. Korsmeyer- Peppas fitting for the release of FA-loaded NPs.